THE ASTROPHYSICAL JOURNAL, 175:77–88, 1972 July 1

THE ABNORMALLY METAL-RICH GLOBULAR CLUSTER NGC 6352

F. D. A. HARTWICK*
University of Victoria

AND

JAMES E. HESSER
Observatorio Inter-Americano de Cerro Tololo†
Received 1971 December 16; revised 1972 February 3

ABSTRACT

A color-magnitude (C-M) diagram has been constructed for the globular cluster NGC 6352 from photoelectric UBV measurements to $V \approx 19$ for 63 stars and from photographic B, V measurements of 397 stars on five or more plate pairs. The C-M diagram, which has been found to be comparable to those of 47 Tucanae and M71, confirms the integrated photometry of van den Bergh and indicates that NGC 6352 is indeed metal rich. A blue "straggler" sequence is also identified. We derive the following properties for NG3 6352: $E_{B-V} = 0.32 \pm 0.05$ mag, $(m - M)_0 = 13.5 \pm 0.3$ mag, and $[\mathrm{Fe/H}] \geq +0.1 \pm 0.1$. Thus NGC 6352 is likely the metal-richest globular cluster known at this time.

I. INTRODUCTION

The basic properties of halo globular clusters have been known for some time (Arp 1955; Sandage 1970), but relatively little work has been done on the so-called metal-rich globular clusters that, in general, are found at low galactic latitudes. Yet it is important to investigate the ensemble of metal-rich globular clusters, despite the observational difficulties imposed by their locations toward the galactic center, as they are possible connecting links between halo objects and the oldest disk objects like M67 and NGC 188. More specifically, the metal abundance of the metal-richest globular clusters should indicate the extent of the enrichment of the interstellar medium within the collapse time of the halo to the disk, a time thought to be $\sim 2 \times 10^8$ years (Eggen, Lynden-Bell, and Sandage 1962). The first color-magnitude diagrams for metal-rich globular clusters were for NGC 6356 (Sandage and Wallerstein 1960)[1] and 47 Tucanae (Wildey 1961; Tifft 1963). Subsequent investigations have provided C-M diagrams for NGC 6723 (Gascoigne and Ogston 1963), NGC 6171 (Sandage and Katem 1964), NGC 6712 (Sandage and Smith 1966), M69 (Hartwick and Sandage 1968), and M71 (Arp and Hartwick 1971).

Spectroscopic surveys of the integrated light of globular clusters carried out by Mayall (1946), Morgan (1956, 1959), and Kinman (1959) revealed a large range in integrated spectral types, indicating a wide variance in metallic line strength; in particular, Mayall (1946) noted the concentration of clusters of later spectral types in the direction of the galactic center. Unfortunately, for many clusters, particularly in the southern hemisphere, no integrated spectral types are available. Therefore, in order to obtain candidates for extreme metal richness for detailed investigation, we made use of the metallicity parameter Q measured by van den Bergh (1967). NGC 6352 [$\alpha(1950) = 17^{\mathrm{h}}21^{\mathrm{m}}.6$, $\delta(1950) = -48°26'$; $l^{\mathrm{II}} = 342°$, $b^{\mathrm{II}} = -7°$] has a Q of -0.09, which is the largest for

* Visiting Astronomer, Cerro Tololo Inter-American Observatory.

† Operated by the Association of Universities for Research in Astronomy, Inc., under contract with the National Science Foundation.

[1] Earlier references to this and the other clusters mentioned herein, may be found in the recent papers cited, and in Alter, Balázs, and Ruprecht (1970) and White (1970).

any cluster in van den Bergh's list. For this reason a photometric program involving a combination of photoelectric and photographic *UBV* observations was initiated on NGC 6352 in 1969 May. Very recently a photometric study of NGC 6352 has been presented by Alcaino (1971). Our investigation extends to much fainter magnitudes, and we believe that the resultant color-magnitude array represents an improvement over that of Alcaino, who considerably extrapolated his photographic measurements beyond the available photoelectric sequence.

II. OBSERVATIONAL DATA

a) *Photoelectric Sequences*

Secondary photoelectric standards were set up around NGC 6352 by using refrigerated, 1P21, single-channel photometers equipped with standard *UBV* filters on the 16-inch and 36-inch (41 and 91 cm) telescopes at Cerro Tololo. Each of the 10 secondary standards were directly tied into the *UBV* system on seven or more nights spread over two observing seasons using a list of standards in current use at Cerro Tololo[2] taken from Cousins and Stoy (1963) and Cousins, Lake, and Stoy (1966); observations of the stars on many (typically, eight) additional nights lends confidence to the values reported herein. The transfer standards are identified in figure 1 (plate 1), and their photoelectric magnitudes and colors are given in table 1. Average internal standard errors in the means of table 1 are $\sigma_V = \pm 0.011$ mag, $\sigma_{B-V} = \pm 0.005$ mag, $\sigma_{U-B} = \pm 0.010$ mag. These secondary standards were then used to calibrate the fainter sequences obtained primarily with the 60-inch (152 cm) telescope; observations of the fainter sequence stars were also tied in to the *UBV* system with the aid of a network of 14 secondary standards set up by the authors near NGC 2477 (Hartwick *et al.* 1972) and NGC 4372 (Hartwick and Hesser, unpublished). As for the original observations of the transfer standards, several different configurations of standard photocells and filters were employed for the photometry of the fainter stars reported here.

The faintest stars in the cluster sequence were chosen from long-exposure plates and in most cases well away from the cluster center to reduce crowding problems in this dense star field. As much care was taken in choosing nearby positions to measure the sky as was taken in choosing the stars. For most of the faint 60-inch photometry a 10″ diaphragm was used. In general, following the philosophy of Gascoigne (1966), we observed the faintest stars on only one or two nights rather than concentrating on a smaller number of stars observed repeatedly. Offset coordinates measured relative to nearby bright stars on our plates were used to obtain magnitudes and colors of stars fainter than $V \sim 17.5$. The observing procedure for these faint stars was normally as follows. Using 1-minute integrations while the star was within sec $Z = 0.1$ of the meridian, we observed V_*, $V_{\rm sky}$, V_*, $V_{\rm sky}$, B_*, $B_{\rm sky}$, B_*, $B_{\rm sky}$, and repeated the sequence three to five times. Sky

TABLE 1

PHOTOELECTRIC MAGNITUDES AND COLORS FOR THE BRIGHT SECONDARY STANDARDS IDENTIFIED IN FIGURE 1

Star	V	$B-V$	$U-B$	n	Star	V	$B-V$	$U-B$	n
A.....	7.04	0.48	0.01	8	F.....	7.56	1.03	0.80	8
B.....	8.82	0.81	0.40	8	G....	9.98	1.58	1.98	9
C.....	10.48	1.56	1.62	7	H....	9.80	0.35	0.13	8
D.....	9.22	0.96	0.67	8	I.....	10.14	0.43	0.02	9
E.....	9.36	1.82	1.99	9	J.....	12.88	0.57	0.19	3

[2] The criteria by which the list of *UBV* standards was selected have been given elsewhere (Hartwick, Hesser, and McClure 1972).

measurements within each filter were generally in different directions, and normally no U-magnitude was measured for these stars. The raw photoelectric data, obtained on strip-chart recordings, were reduced using the current Kitt Peak National Observatory UBV reduction program. Magnitudes and colors for the 63 photoelectric standards observed around NGC 6352 are given in table 2, while identification is provided in figure 1.

b) Photographic Measurements

More than 20 plates of NGC 6352 in V (103aD + GG14) and B (103aO + GG13) were obtained with the f:7.5 Ritchey-Chrétien focus of the 60-inch reflector. The material spread over two observing seasons, during which time the collimation of the telescope was noticeably improved. Exposure times ranged from 15 to 60 minutes. Following measurements with a Cuffey-style iris photometer, two methods of reducing the photographic material were tried. The first way was to reduce all iris readings to one plate, average them, and then plot a calibration curve from which magnitudes were read. The second method was to plot a calibration curve for each plate separately and average the resulting magnitudes. Both methods gave the same result; and the second method, for which error estimation is more straightforward, was used for all the data. The calibration curves were sixth-degree polynomials fitted by machine least squares. The stars measured photographically are identified in figure 2 (plate 2), and their magnitudes and colors are listed in table 3. Approximately 400 stars—essentially all for which careful visual inspection showed that there existed no obvious crowding or overlapping problems—were measured, and in figure 3 we present all the photographic observations. Median internal standard errors for stars brighter than $V \sim 17$ are: ± 0.01 in V and ± 0.02 in $(B - V)$; while for stars fainter than $V \sim 17$ these errors are: ± 0.04 in V and ± 0.07 in $(B - V)$.

TABLE 2

PHOTOMETRIC DATA FOR THE FAINT SEQUENCE STARS IDENTIFIED IN FIGURE 1

Star	V_{pe}	$(B-V)_{pe}$	$(U-B)_{pe}$	n_{pe}	V_{pg}	$(B-V)_{pg}$	Star	V_{pe}	$(B-V)_{pe}$	$(U-B)_{pe}$	n_{pe}	V_{pg}	$(B-V)_{pg}$
1	13.25	1.62	2.14	5	13.18	1.70	34	17.57	0.99		1	17.68	0.96
2	12.38	0.66	0.12	5	12.42	0.59	35	16.21	1.05		1	16.14	1.11
3	15.80	1.22	1.27	1	15.69	1.20	36	17.05	0.84		2	16.89	0.88
4	14.14	0.73	0.27	3	14.11	0.67	37	14.65	0.56	0.19	3	14.73	0.43
5	12.05	1.56	1.94	4	12.06	1.61	38	14.20	0.73	0.21	1	14.24	0.60
6	15.95	0.61	0.12	2	15.97	0.58	39	15.76	0.95		1	15.85	0.86
7	12.80	1.49	1.82	5	12.81	1.52	40	13.61	1.53	1.76	2	13.60	1.57
8	11.66	1.51	1.82	5	11.66	1.60	41	17.19	1.24		1	17.10	1.39
9	12.06	1.21	1.08	4	12.00	1.23	42	13.24	1.68	2.15	2	13.22	1.82
10	12.20	0.61	0.19	4	12.28	0.54	43	15.90	0.99		1	15.93	1.00
11	10.98	0.42	0.07	5	10.99	0.42	44	15.07	1.07	0.73	1	15.10	1.06
12	16.78	0.89	1.07	1	16.80	0.91	45	17.97	0.96		1	18.05	0.82
13	13.86	1.11	0.83	2	13.81	1.10	46	16.35	1.29	1.72	2	16.34	1.34
14	15.28	1.30	1.63	1	15.29	1.29	47	14.45	1.64	2.02	2	14.40	1.78
15	15.78	1.23	1.19	1	15.89	1.30	48	16.81	0.89	0.87	2	16.88	0.92
16	16.36	1.33	0.95	1	15.89	1.32	49	17.61	0.79		1	17.49	0.88
17	12.92	1.69	1.84	5	12.76	1.71	50	18.20	0.85		1	18.23	1.00
18	13.54	1.87	2.44	2	13.45	1.88	51	17.31	1.04		1	17.27	1.05
19	15.77	0.70	0.32	1	15.54	0.67	52	18.10	0.60		1	17.83	0.72
20	19.00	1.27		1	18.32	1.20	53	19.22	0.75		1	18.86	1.12
21	14.52	1.41	1.42	3	14.54	1.45	54	15.16	0.77	0.20	1	15.29	0.65
22	14.09	1.62	1.93	2	14.07	1.70	55	18.42	1.24		1	18.61	0.84
23	17.59	0.96		1	17.69	0.91	56	18.23	0.87		2	18.69	0.95
24	12.63	0.58		1	12.80	0.47	57	13.53	1.43		1	13.62	1.44
25	17.99	0.98		1	18.17	0.89	58	14.07	1.36	1.41	1	14.07	1.41
26	16.84	0.79		2	16.93	0.71	59	16.32	1.37		1	16.33	1.42
27	15.18	1.13	1.07	3	15.22	1.16	60	13.43	1.76		1	13.60	1.80
28	16.69	0.76		2	16.76	0.73	61	13.20	1.37		1	13.22	1.40
29	15.86	1.41		2	15.93	1.47	62	15.82	0.86	0.66	1		
31	17.89	0.82		1	18.09	0.82	63	13.66	0.93	0.62	1		
32	17.37	0.87		1	17.51	0.73	64	14.94	1.32	0.80	1		
33	14.92	1.74	2.36	2	14.88	1.94							

TABLE 3

PHOTOGRAPHICALLY DETERMINED MAGNITUDES AND COLORS FOR THE

PROGRAM STARS IDENTIFIED IN FIGURE 2

Star	V	B-V	Star	V	B-V	Star	V	B-V	Star	V	B-V
1	15.03	1.32	49	16.81	1.11	117	16.71	1.14	161	13.60	1.80
2	16.32	1.15	50	14.86	1.05	118	15.01	1.34	162	14.25	1.57
4	16.18	1.17	51	15.20	0.55	119	16.82	1.08	163	14.74	1.41
5	16.17	1.14	52	14.86	1.02	121	14.62	1.20	164	15.81	1.28
7	15.68	0.74	53	15.41	1.22	122	16.36	1.17	165	16.62	1.20
8	15.48	1.13	54	16.13	0.82	123	16.97	0.66	166	16.54	1.22
9	15.50	1.21	55	13.03	1.87	124	15.67	1.24	167	15.21	1.14
10	14.96	1.07	56	15.03	1.02	125	15.16	1.00	168	16.73	1.11
11	15.55	1.16	57	15.64	1.20	126	16.28	1.32	169	16.25	1.23
12	14.07	1.56	59	14.79	0.48	127	16.91	0.82	170	16.12	1.35
13	16.40	1.01	60	14.80	1.20	128	12.69	0.43	171	15.46	1.26
14	15.61	1.25	61	15.94	1.13	129	14.10	1.38	173	15.39	0.65
15	16.49	1.12	62	14.97	0.71	130	16.17	0.75	174	16.05	1.18
16	16.74	1.07	63	14.80	1.08	131	16.48	1.13	175	16.53	1.21
17	16.60	1.10	64	15.66	1.41	132	15.82	0.64	176	16.59	1.23
18	16.48	1.14	65	15.22	1.17	133	16.77	1.07	177	17.27	1.09
19	15.06	1.02	66	16.65	1.23	134	16.43	0.65	178	17.39	1.27
20	15.02	1.12	67	15.04	1.09	135	12.64	0.60	179	15.54	1.22
21	16.03	1.04	69	15.48	1.24	136	16.15	1.25	180	15.43	0.70
23	17.13	1.00	70	15.52	1.14	137	16.99	0.90	181	13.83	1.63
24	16.61	1.08	71	15.62	1.21	139	17.18	0.84	182	15.70	1.32
25	16.42	1.16	72	14.01	1.47	140	16.08	1.20	183	15.21	1.31
26	16.69	1.19	73	14.60	1.07	141	16.14	1.17	184	15.88	1.21
27	16.19	1.15	74	16.59	0.72	142	14.27	1.51	185	16.05	1.34
30	16.63	1.12	75	14.49	1.36	143	16.51	1.13	186	14.74	1.38
31	15.63	1.13	101	17.12	0.99	144	16.48	1.16	187	13.20	1.93
32	15.01	1.20	102	16.02	0.72	145	16.34	1.04	188	16.55	1.27
33	14.87	1.28	103	16.78	0.73	146	16.06	1.18	189	16.50	1.39
34	15.70	1.28	104	15.01	1.05	147	17.04	1.17	190	13.66	1.62
35	14.90	0.47	106	15.56	1.22	148	16.44	1.13	191	15.21	1.16
36	16.49	1.05	107	16.86	1.07	149	15.26	1.01	192	15.26	1.31
37	13.01	1.86	108	17.29	1.00	150	15.20	1.13	193	15.96	0.73
38	16.10	0.37	109	16.86	1.29	151	16.60	1.39	194	16.12	0.76
40	14.81	1.25	110	16.92	1.04	154	15.15	1.02	195	15.34	1.15
41	15.22	0.98	111	14.33	1.41	155	15.27	1.16	196	16.33	1.14
42	15.57	1.26	112	15.37	1.54	156	15.73	1.59	200	15.83	1.30
43	15.62	1.29	113	13.12	2.04	157	15.93	1.21	201	15.29	1.10
44	15.06	1.05	114	15.82	1.41	158	16.38	1.22	202	15.30	1.15
46	14.65	1.39	115	16.80	0.88	159	15.54	1.26	203	14.94	1.10
48	14.61	1.47	116	16.53	1.38	160	15.23	1.07	204	16.91	1.16

TABLE 3—continued

Star	V	B−V	Star	V	B−V	Star	V	B−V	Star	V	B−V
205	15.26	1.05	248	15.36	1.78	336	18.44	0.89	380	17.66	0.46
206	16.23	1.18	249	16.33	1.14	337	18.71	0.94	381	17.99	1.14
207	17.05	0.97	250	15.15	1.04	338	18.15	0.96	382	17.76	1.16
208	16.84	0.89	251	16.72	1.11	339	18.61	0.77	384	18.02	1.19
209	16.38	0.86	252	15.03	1.09	340	18.22	0.88	385	18.02	1.25
210	16.86	1.25	253	15.12	1.04	341	18.32	1.00	386	17.90	1.18
211	14.58	1.55	254	14.16	0.88	342	17.68	1.15	387	17.46	1.01
212	16.41	1.25	255	16.66	1.05	343	18.51	0.99	388	16.62	1.01
213	15.00	1.19	256	15.26	1.11	344	17.88	1.05	390	17.83	1.24
214	15.72	1.25	257	15.11	1.11	345	18.30	1.02	391	16.72	1.34
215	16.49	0.84	302	17.89	0.56	346	17.72	1.01	392	17.04	1.19
216	16.81	0.87	303	17.74	1.27	347	18.11	1.10	393	17.61	1.14
217	16.91	0.84	304	17.83	1.28	348	18.25	1.02	394	18.02	1.31
218	16.39	1.16	305	17.73	1.19	349	18.67	0.73	395	17.37	1.43
219	15.63	1.55	306	17.48	1.13	350	18.45	0.94	397	17.39	1.00
220	15.16	1.14	307	17.92	1.20	351	17.20	1.19	398	17.12	1.17
221	16.29	1.13	309	17.97	1.05	353	18.13	0.86	399	18.07	1.02
224	15.65	0.66	310	18.35	0.74	354	17.97	1.04	400	17.34	0.57
225	17.19	1.23	311	17.26	0.86	355	18.45	1.03	401	18.22	1.14
226	16.18	1.10	313	17.83	1.23	356	16.89	1.25	402	16.80	1.23
227	16.79	0.93	314	18.26	1.00	357	18.56	0.88	403	18.22	0.88
228	16.41	1.13	315	18.29	0.99	358	17.36	0.91	404	17.35	1.09
229	15.67	0.84	316	18.35	1.00	359	17.87	1.05	405	17.42	0.58
230	17.18	1.07	317	18.57	0.98	360	18.47	1.15	406	18.27	1.14
231	15.93	1.14	318	17.91	1.06	361	17.34	0.96	407	17.67	1.00
232	16.57	0.89	319	18.34	0.91	362	18.14	1.34	408	18.46	0.99
233	14.89	1.17	320	18.26	0.87	363	18.05	1.32	409	18.74	0.91
234	15.14	1.07	321	17.85	1.26	364	17.48	1.22	410	18.64	1.03
235	16.76	1.26	323	17.84	1.05	365	18.88	0.90	411	17.12	1.20
236	15.23	1.03	324	17.20	1.20	366	17.17	1.30	413	18.02	1.22
237	15.19	0.99	325	18.02	1.07	367	17.96	0.96	414	17.46	1.11
238	16.11	1.15	326	17.52	0.82	368	18.40	1.21	415	17.53	1.09
239	15.72	1.12	327	17.54	0.96	369	17.76	0.89	417	18.20	1.07
240	16.25	0.87	328	17.92	1.15	370	17.76	0.99	419	18.13	1.14
241	15.66	1.18	329	17.80	1.09	371	18.08	1.44	420	18.17	0.94
242	16.38	0.82	330	18.52	0.91	373	17.06	1.27	422	17.14	0.83
243	15.89	0.81	331	17.57	1.14	374	18.34	0.88	423	18.16	0.96
244	16.26	1.03	333	17.64	1.16	375	17.18	1.20	425	18.11	1.06
245	15.09	0.98	334	17.43	1.00	376	17.84	1.07	426	18.48	0.54
246	16.14	0.85	335	17.03	0.84	379	17.26	1.24	428	18.11	0.87

TABLE 3—continued

Star	V	B-V	Star	V	B-V
429	17.11	1.20	474	18.55	0.86
430	17.13	0.94	475	18.04	0.93
431	18.62	0.93	476	17.66	0.96
432	18.12	1.02	479	17.99	0.86
433	16.94	1.21	478	17.91	0.86
434	16.90	1.23	479	17.92	1.03
435	17.76	1.29	480	18.46	0.86
437	17.92	1.07	481	18.19	1.09
438	17.67	1.18	482	18.16	1.27
439	17.55	1.21	483	18.55	0.81
440	18.06	1.09	484	17.22	1.05
442	17.40	0.99	485	17.93	0.88
443	17.70	1.00	486	16.89	1.10
444	18.83	1.05	487	17.23	1.06
445	18.63	0.88	488	17.59	1.40
446	18.29	0.94	489	17.33	1.16
447	18.62	0.81	490	17.57	1.16
448	18.40	0.96	491	18.54	1.04
449	18.06	0.94	492	18.53	1.01
451	17.98	0.71	493	18.77	1.04
452	18.03	0.82	494	18.58	1.02
453	18.03	0.93	495	18.64	0.73
454	18.05	1.05	496	18.31	1.08
455	17.58	0.90	497	18.64	1.06
456	18.57	0.87	498	18.30	0.91
457	17.61	1.22	499	18.48	0.90
459	18.16	0.93	500	18.61	0.96
460	18.13	1.07	501	18.26	0.89
461	18.43	0.89	502	18.12	0.97
462	18.27	1.20	503	18.03	1.03
464	18.36	0.83	504	18.32	1.03
465	18.20	0.97	505	18.31	1.09
466	18.47	0.99	506	18.47	0.83
467	18.61	0.76	507	18.59	0.95
468	18.33	0.93	508	18.62	1.07
469	18.53	0.88	509	18.54	1.12
470	18.26	0.89	510	18.43	0.96
471	18.47	0.79			
472	17.21	0.71			
473	18.30	0.91			

A further consideration which entered into the selection of the photoelectric standards was that they be chosen in such a manner that a check could be made for field errors in the photographic data. The differences $(V_{pe} - V_{pg})$ and $(B_{pe} - B_{pg})$ were checked for systematic trends as a function of position on the plate. No significant trend was noted on any particular groups of plates. Although field errors of $\sim \pm 0.06$ mag within $12'$ of the plate center cannot be directly ruled out by our data, observations made under similar conditions of telescope collimation of the open cluster NGC 2477 (Hartwick, Hesser, and McClure 1972) failed to find field errors ≥ 0.03 mag in a similar area of the plates. A check was also made for color equations in the photographically determined magnitudes and no significant ones were found. Finally, a crude estimate of how the photometric accuracy behaves within successively fainter magnitude ranges can be made by using the differences in photoelectrically and photographically determined values: (i) $V \leq 16.0$, $|\langle V_{pe} - V_{pg}\rangle| = 0.06$ mag, $|\langle (B - V)_{pe} - (B - V)_{pg}\rangle| = 0.06$ mag; (ii) $16.0 < V \leq 18.0$, $|\langle V_{pe} - V_{pg}\rangle| = 0.11$ mag, $|\langle (B - V)_{pe} - (B - V)_{pg}\rangle| = 0.06$ mag; and (iii) $V > 18.0$, $|\langle V_{pe} - V_{pg}\rangle| = 0.33$ mag, $|\langle (B - V)_{pe} - (B - V)_{pg}\rangle| = 0.20$ mag. No photographic "smoothing" has been applied to any of the data in this paper.

III. THE COLOR-MAGNITUDE DIAGRAM AND DETERMINATION OF THE REDDENING

The C-M diagram shown in figure 3 for NGC 6352 is very similar to that of 47 Tucanae (Tifft 1963) and M71 (Arp and Hartwick 1971) with respect to: (i) the slope of the giant branch, (ii) the existence of only a stubby red horizontal branch, (iii) the break in the giant branch at the horizontal branch, and (iv) the blue-straggler sequence. Clearly, then, NGC 6352 is a member of the class of metal-rich globular clusters, as suggested by van den Bergh's (1967) photometry.

In order that an estimate of [Fe/H] can be made, a knowledge of the reddening is required. This problem is complicated by the lack of any of the very blue horizontal-branch stars that are commonly found in halo clusters. We have estimated E_{B-V} for NGC 6352 in the following two ways. The first consists in superposing the C-M diagram of 47 Tucanae on figure 3. The horizontal shift required is 0.35 mag, and with $E_{B-V} = 0.02$ mag for 47 Tucanae, we find $E_{B-V} = 0.37$ mag for NGC 6352. The problem with this method is the implicit assumption that the C-M diagram of 47 Tucanae and NGC 6352 are the same, implying identical chemical composition. We will show in § V that NGC 6352 is metal richer than 47 Tucanae and as such should have a redder giant branch. For this reason, we consider the value of 0.37 mag to be an upper limit for the reddening of NGC 6352.

The reddening of the cluster may also be estimated from observations of field stars around the cluster. Table 4 gives observations of 11 stars in the vicinity of NGC 6352. The stars are identified by their number in the *Smithsonian Astrophysical Observatory Star Catalog*. The spectral types given in table 4 are also taken from this catalog. We assumed that each star was a main-sequence star and deduced the reddening and distance modulus given in table 4. We note that our assumption will result in an overestimate of the reddening and an underestimate of the distance modulus should the star be evolved. The data in table 4 are plotted in figure 4, and, for the reasons just discussed, we have drawn a straight line through the lowest points. The slope of this line represents $A_B = 1.3$ mag kpc^{-1}. The observations in table 4 do not go sufficiently faint for a leveling off of the reddening to become apparent in figure 5. However, on the basis of a dis-

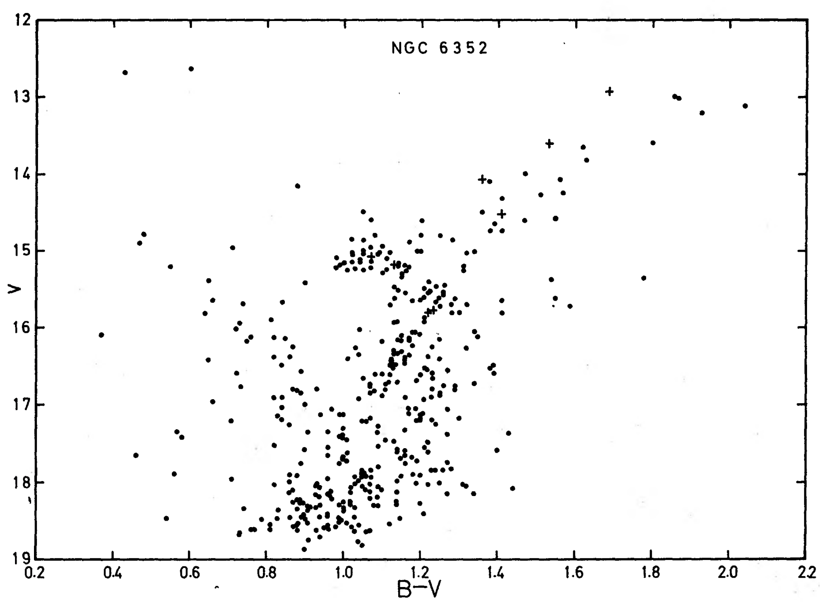

FIG. 3.—The color-magnitude diagram for ~400 stars measured near NGC 6352. Crosses are photoelectric data from table 2 for stars which are considered to be cluster members.

DATA FOR STARS USED TO ESTIMATE THE REDDENING TOWARDS NGC 6352

Star	Sp Type	V	B-V	U-B	E_{B-V}	$(B-V)_0$	V_0	M_V	r (pc)
227923	B5	6.75	0.09	-0.61	0.33	-0.24	5.76	-1.90	340
227927	B8	9.30	0.09	-0.25	0.21	-0.21	8.67	+0.30	472
227928	B9	9.35	0.07	-0.09	0.13	-0.06	8.96	+1.07	378
227931	A0	8.76	0.01	-0.30	0.12	-0.11	8.40	+0.43	392
227944	B8	6.90	-0.06	-0.59	0.14	-0.20	6.48	-1.10	328
227815	B9	6.66	0.61	0.09	0.72	-0.12	4.50	+0.30	69
227819	B8	8.53	0.02	-0.41	0.18	-0.16	7.99	-0.38	472
227843	A0	7.24	0.10	0.06	0.11	-0.01	6.89	+1.48	121
228015	B5	7.61	-0.06	-0.53	0.12	-0.18	7.25	-0.66	382
228061	A2	9.01	0.35	-0.22	0.51	-0.17	7.48	-0.51	396
228097	B8	9.26	0.08	-0.38	0.24	-0.16	8.54	-0.38	608

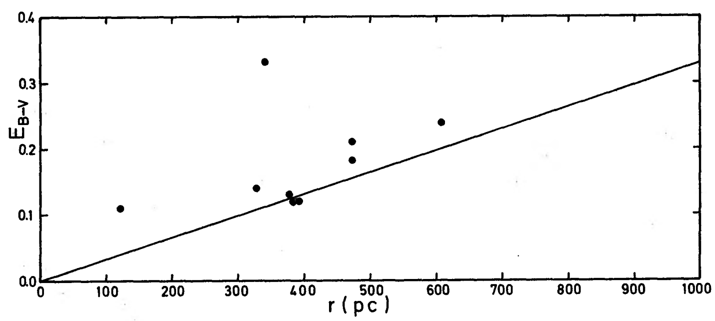

FIG. 4.—A plot of reddening against distance for field stars in the vicinity of NGC 6352. Data are taken from table 4.

cussion by Arp (1965), we have adopted an absorption layer thickness of 100 pc, which the line of sight to NGC 6352 intersects at a distance of 820 pc. From figure 5 the reddening at this distance is $E_{B-V} = 0.27$ mag, and we consider this to be a lower limit to the reddening of NGC 6352. The mean of the lower and upper limits gives our adopted reddening of $E_{B-V} = 0.32 \pm 0.05$ mag. Inspection of the photographic plates fails to reveal indications of strong differential reddening, but detailed investigation of more subtle differential effects will have to await future analytical and observational efforts.

IV. FIELD STARS AND THE REALITY OF THE BLUE-STRAGGLER SEQUENCE

Figure 3 shows an apparently well-defined sequence of stars approximately parallel to the zero-age main sequence. Similarly, the C-M diagram of 47 Tucanae by Tifft (1963) shows several "blue straggler" candidates, as does the C-M diagram of M71. However, because NGC 6352 is at low galactic latitude, it is important to know what the contribution of field stars is to this group of stars. We obtained C-M diagrams for stars in areas of 2′ radii located at 8′ and 12′ from the cluster center; the locations of the areas chosen are shown in figure 1. Inspection of the C-M diagrams for the two areas, presented in figure 5, shows little trace of either a horizontal or giant branch.

Since at this time we lack alternative, preferably spectroscopic, means for ascertaining the cluster membership of these blue stragglers, we have adopted a simple statistical approach based upon star counts to clarify the reality of their membership. Counts were

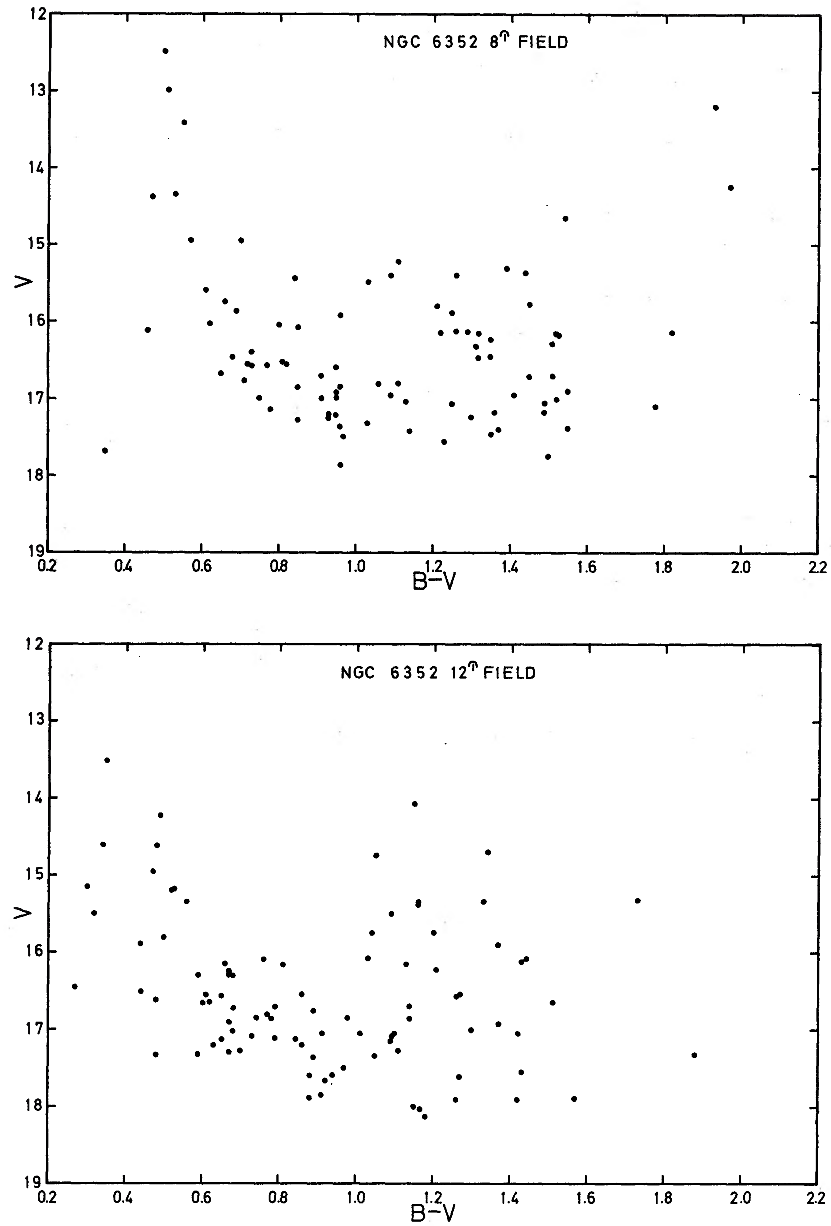

FIG. 5.—C-M diagrams determined for the two control areas of the general field surrounding NGC 6352 (fig. 1). As discussed in § IV, combined photometry and star counts in these fields lend strong confirmation to the reality of the identification of a pronounced blue-straggler sequence in NGC 6352.

made of stars in these areas brighter than $V = 16.5$ and bluer than $(B - V) = 0.90$. There were 19 and 21 such stars in the 8′ and 12′ fields, respectively, compared to 26 such stars which were measured within 2′ of the cluster center; but the latter number is incomplete due to crowding. Approximate completeness factors were conservatively estimated by further counting the number of stars that were not measured in the iris photometry (due to problems of crowding, etc.) and comparing those results with the number of stars measured by iris-photometric techniques within each area; those counts revealed an $\sim$41 percent completeness to $V = 16.5$ within 1′ of the cluster center and $\sim$ 79 percent completeness in the 1′–2′ annulus. When the numbers of stars measured are adjusted by these figures, the total number of blue stars within 2′ of the cluster center is estimated to be 41 ± 10, which is approximately twice the number found in the field. We conclude that the blue-straggler sequence in NGC 6352 is real; however, more definite confirmation via spectroscopic means is clearly desirable.

V. THE TWO-COLOR DIAGRAM AND AN ESTIMATE OF [Fe/H]

A two-color diagram for stars thought to be members of NGC 6352 is shown in figure 6. The plotted points are photoelectric measurements from table 2 corrected for reddening according to procedures that take into account the steepened reddening line for stars near $(B - V)_0 = 1.0$, as outlined by Hartwick and McClure (1972). The line through each point represents the shift due to ±0.05 mag uncertainty in the reddening. Several of the stars lie up to 8′ from the cluster center, and their membership is uncertain. The criterion for selection of stars for inclusion in figure 6 is that they fall on or near the principal sequences in figure 3. Assuming that these stars are members, we find $\delta(U - B)_{B-V=1.0} = -0.1 \pm 0.1$ mag, implying $[\mathrm{Fe/H}]_{\mathrm{NGC\,6352}} \geq [\mathrm{Fe/H}]_{\mathrm{Hyades}}$. Thus NGC 6352 appears to have the highest metal abundance for any globular cluster investigated to date.

Relevant properties of other metal-rich globular clusters for which an estimate of [Fe/H] has been made are summarized in table 5 for comparison with the present results. $(B - V)_{0,g}$ represents the color of the giant branch at the magnitude of the horizontal branch, and Q is the metallicity parameter measured by van den Bergh (1967). Unfortunately we must emphasize the uncertainty in the value of [Fe/H] deduced for NGC 6352 because of (i) uncertainty of membership of the stars considered in figure 6 and (ii) uncertainty in the measured $(U - B)$ values. Comparison of the data in table 5 nevertheless emphasizes the high metal content of NGC 6352.

VI. AN ESTIMATE OF THE DISTANCE TO NGC 6352

The turnoff in NGC 6352 may have been reached by our photometry in figure 3, but the uncertainties of V and $B - V$ measures with a 60-inch telescope at $V \gtrsim 18.0$ com-

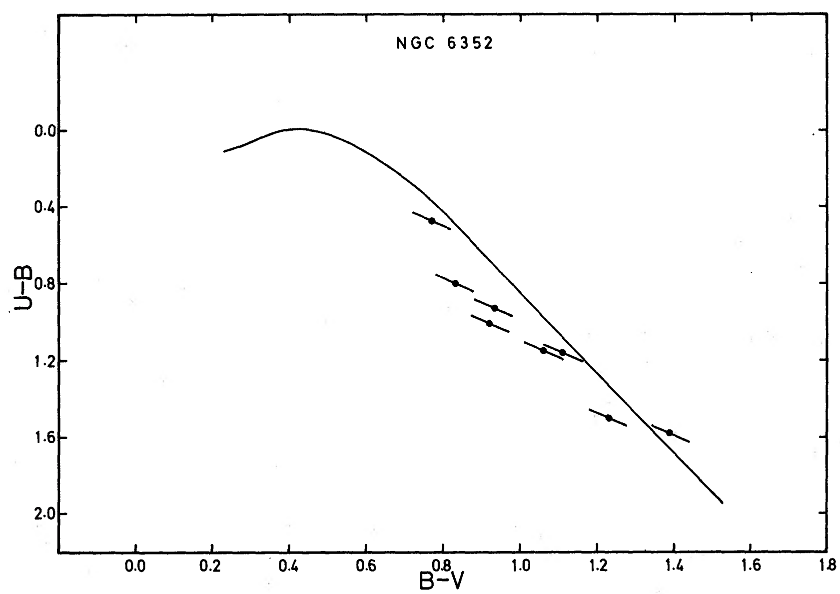

FIG. 6.—The two-color diagram for those stars in table 2 considered to be cluster members. As explained in the text, the points have been corrected for reddening, and the line through each point shows the shift due to uncertainty in the reddening of ±0.05 mag.

TABLE 5

SOME PROPERTIES OF THREE METAL-RICH GLOBULAR CLUSTERS

Cluster	Reddening	$(B-V)_{0,g}$	Sp Type	Q	Fe/H	Ref. for Fe/H
47 Tucanae.......	0.02	0.90	G3	−0.26	>-0.6	1
M71.............	0.31	0.89	G6	−0.23	~-0.3	2
NGC 6352........	0.32	0.98	...	−0.09	$\gtrsim+0.1$	3

REFERENCES—(1) Feast and Thackeray 1960; (2) Arp and Hartwick 1971; (3) this paper.

bined with the low galactic latitude of the cluster makes the identification of the turnoff a speculative venture at best. Not only does our inability to delineate reliably the turnoff prevent us from estimating the age of the cluster from a comparison with theoretical tracks, but the main-sequence fitting technique for obtaining the distance modulus is inapplicable. Furthermore, there are no known RR Lyrae variables in the cluster by which the distance may be estimated. Instead, we assume that the horizontal branches in 47 Tucanae and NGC 6352 have the same absolute magnitude. With $(m - M)_{0,47\ \mathrm{Tuc}} =$ 13.3 mag (Tifft 1963), we find $(m - M)_{0,\mathrm{NGC}\ 6352} = 13.5 \pm 0.3$ mag, corresponding to a distance of 5 kpc at 0.6 kpc below the galactic plane.

VII. CONCLUSIONS

From this photometric study of the globular cluster NGC 6352 we find:

i) Confirmation of the extreme metal-richness indicated by integrated photometry. The topology of the C-M diagram is similar to that of other metal-rich clusters, although the giant branch of NGC 6352 is even redder than that of 47 Tucanae.

ii) The cluster contains a blue-straggler sequence and the C-M array shows a sudden decrease in the number of giants at $\sim$0.2 mag below the horizontal branch.

iii) NGC 6352 is characterized by $E_{B-V} = 0.32 \pm 0.05$ mag, $(m - M)_0 = 13.5 \pm 0.3$ mag, and $[\mathrm{Fe/H}] \geq +0.1 \pm 0.1$.

The metal abundance inferred from the ultraviolet excess of the giant stars in NGC 6352 is abnormally high. Should future observations confirm this result, an interesting puzzle emerges. The $(B - V)_{0,g}$ values for the old open clusters NGC 188 and NGC 6791 are approximately 0.2–0.3 mag redder than the value for NGC 6352, yet the metal abundances are approximately the same. A similar situation exists for the halo globular clusters, where a range in $(B - V)_{0,g}$ for clusters with the same metal abundances has been found (Hartwick 1968). It is tempting to speculate that the same Y parameter in Hartwick's (1968) scheme is responsible for the above discrepancy, such that $Y_{\mathrm{NGC}\ 6352} > Y_{\mathrm{NGC}\ 188}$. Clearly it would be desirable to obtain spectra and/or narrow-band photometry of individual stars in NGC 6352 to confirm the high [Fe/H] ratio found in this investigation.

We wish to thank Mr. S. Becklake and Mrs. M. Reeves for measuring many of the plates and Mrs. J. V. Barnes and Mrs. B. Weyman for their extensive assistance during the photoelectric reductions. This work would not have been accomplished with so few observational problems were it not for the excellent help provided by the Cerro Tololo night assistants; we particularly thank Srs. C. Bolelli, E. Figueroa, A. Gomez, R. González, O. Saá and P. Zamorano. We are also grateful to the National Science Foundation for their support of the Cerro Tololo Inter-American Observatory. One of us (F. D. A. H.) acknowledges financial support from the University of Victoria and the National Research Council of Canada.

REFERENCES

Alcaino, G. 1971, *Astr. and Ap.*, **11**, 7.
Alter, G., Balázs, B., and Ruprecht, J. 1970, *Catalog of Star Clusters and Associations* (Budapest: Akademiai Kiadó).
Arp, H. C. 1955, *A.J.*, **60**, 317.
———. 1965, *Ap. J.*, **141**, 43.
Arp, H. C., and Hartwick, F. D. A. 1971, *Ap. J.*, **167**, 499.
Bergh, S. van den. 1967, *A.J.*, **72**, 70.
Cousins, A. W. J., Lake, R., and Stoy, R. H. 1966, *R.O.B.*, No. 121.
Cousins, A. W. J., and Stoy, R. H. 1963, *R.O.B.*, No. 64.
Eggen, O., Lynden-Bell, D., and Sandage, A. 1962, *Ap. J.*, **136**, 748.
Feast, M. W., and Thackeray, A. D. 1960, *M.N.R.A.S.*, **120**, 463.
Gascoigne, S. C. B. 1966, *M.N.R.A.S.*, **134**, 59.
Gascoigne, S. C. B., and Ogston, F. A. 1963, *Observatory*, **83**, 64.
Hartwick, F. D. A. 1968, *Ap. J.*, **154**, 475.
Hartwick, F. D. A., Hesser, J. E., and McClure, R. D. 1972, *Ap. J.*, **174**, 557.
Hartwick, F. D. A., and McClure, R. D. 1972, *Pub. A.S.P.*, **84**, 288.
Hartwick, F. D. A., and Sandage, A. 1968, *Ap. J.*, **153**, 715.
Kinman, T. D. 1959, *M.N.R.A.S.*, **119**, 538.
Mayall, N. U. 1946, *Ap. J.*, **104**, 290.
Morgan, W. W. 1956, *Pub. A.S.P.*, **68**, 509.
———. 1959, *A.J.*, **64**, 432.
Sandage, A. 1970, *Ap. J.*, **162**, 841.
Sandage, A., and Katem, B. 1964, *Ap. J.*, **139**, 1088.
Sandage, A., and Smith, L. L. 1966, *Ap. J.*, **144**, 886.
Sandage, A., and Wallerstein, G. 1960, *Ap. J.*, **131**, 598.
Tifft, W. G. 1963, *M.N.R.A.S.*, **126**, 209.
Wildey, R. L. 1961, *Ap. J.*, **133**, 430.
White, R. E. 1970, *Ap. J. Suppl.*, **19**, 343.